



THE UNIVERSITY *of* EDINBURGH

Edinburgh Research Explorer

## Geochemical interactions in geological hydrogen Storage: The role of sandstone clay content

**Citation for published version:**

Al-Yaseri, A, Yekeen, N, Al-Mukainah, H & Hassanpouryouzband, A 2024, 'Geochemical interactions in geological hydrogen Storage: The role of sandstone clay content', *Fuel*, vol. 361, 130728. <https://doi.org/10.1016/j.fuel.2023.130728>

**Digital Object Identifier (DOI):**

[10.1016/j.fuel.2023.130728](https://doi.org/10.1016/j.fuel.2023.130728)

**Link:**

[Link to publication record in Edinburgh Research Explorer](#)

**Document Version:**

Peer reviewed version

**Published In:**

Fuel

**General rights**

Copyright for the publications made accessible via the Edinburgh Research Explorer is retained by the author(s) and / or other copyright owners and it is a condition of accessing these publications that users recognise and abide by the legal requirements associated with these rights.

**Take down policy**

The University of Edinburgh has made every reasonable effort to ensure that Edinburgh Research Explorer content complies with UK legislation. If you believe that the public display of this file breaches copyright please contact [openaccess@ed.ac.uk](mailto:openaccess@ed.ac.uk) providing details, and we will remove access to the work immediately and investigate your claim.



1 ***Geochemical Interactions in Geological Hydrogen Storage: The Role of Sandstone Clay***

2 ***Content***

3 Ahmed Al-Yaseri<sup>1</sup>, Nurudeen Yekeen<sup>2</sup>, Hani Al-Mukainah<sup>1</sup>, Aliakbar Hassanpouryouzband<sup>3</sup>

4 <sup>1</sup>Center of Integrative Petroleum Research (CIPR), College of Petroleum Engineering and  
5 Geoscience, King Fahd University of Petroleum and Minerals, Saudi Arabia

6 <sup>2</sup>School of Engineering, Edith Cowan University, Joondalup 6027, WA, Australia

7 <sup>3</sup>School of Geosciences, University of Edinburgh, Grant Institute, West Main Road, Edinburgh  
8 EH9 3FE, U.K.

9

10 ***Abstract***

11 Hydrogen holds promise as a clean energy alternative, crucial for achieving global decarbonization  
12 goals and net-zero carbon emissions. Its low volumetric energy density necessitates underground  
13 storage in sandstone formations to maintain year-round supply. The efficacy of such storage hinges  
14 on the geochemical interplay between hydrogen and the host sandstone. Despite the slow reaction  
15 rates in sandstone, the influence of its clay composition on hydrogen interaction remains  
16 underexplored. In this study, we specifically investigate the geochemical interactions of hydrogen  
17 with clay-bearing sandstone formations under controlled conditions, simulating storage scenarios.  
18 This study evaluates the impact of clay on hydrogen-sandstone geochemistry after 75 days of  
19 injection at 1500 psi and 75°C into Berea and Bandera gray sandstone cores, utilizing  
20 microcomputed tomography to assess changes in pore structure. Our results reveal that, even in  
21 sandstones with high clay content, there is negligible alteration in porosity and mineral content  
22 over storage time, indicating stability in these formations. These findings provide crucial insights  
23 for selecting suitable geological formations for hydrogen storage, supporting the global shift

24 towards sustainable energy systems Our study contributes to the global efforts in decarbonization  
25 by providing essential guidance on the feasibility of using clay-bearing sandstone formations for  
26 efficient and sustainable hydrogen storage.

27 **Keywords:** Hydrogen; clay; sandstone; geochemical reactions; underground hydrogen storage.

28  
29 **1. Introduction**

30 Hydrogen is considered a prominent energy carrier, poised to play a significant part in the  
31 energy transition from carbon-based fuel to clean energy and attainment of global decarbonization  
32 pursuit [1-3]. While renewable energy sources have been favored as alternatives to fossil fuels,  
33 their inherent intermittency and seasonal variability limit their reliability [4, 5]. To counter this,  
34 green hydrogen, produced via surplus renewable energy, presents a solution by offering storable  
35 energy that can bridge gaps in supply [6, 7].

36 Nevertheless, there are several hitches that are associated with surface storage, H<sub>2</sub> is highly  
37 flammable with high tendency to mix with air or O<sub>2</sub> when stored at the surface facilities [8, 9]. It  
38 will need just 5% of O<sub>2</sub> for combustion, unlike fossil fuel that will require around 12% to burn. Its  
39 flammability in oxygen has been estimated to vary between 4 to 94%, suggesting that the  
40 occurrence of explosions is likely if surface H<sub>2</sub> storage is not meticulously managed. H<sub>2</sub> also has high  
41 diffusivity, thus the general cost of surface storage installation and maintenance could be quite  
42 outrageous [10, 11].

43 As a result, subsurface geological formations, such as saline aquifers and depleted  
44 hydrocarbon reservoirs, have emerged as preferable options for hydrogen storage. [12, 13]. These  
45 settings offer a safer and more economical alternative, essential for the hydrogen economy, by  
46 facilitating a stable grid and ensuring hydrogen's availability during peak demands [14, 15].

47 Notably, underground storage mitigates explosion risks due to the reduced oxygen levels. While  
48 salt caverns, historically utilized for town and natural gas storage, offer a straightforward structure  
49 and high withdrawal rates, their capacity and durability under cyclic injection remain limited [15,  
50 16]. Additionally, their geographic distribution and proximity to hydrogen production sites present  
51 logistical challenges [17].

52 On the other hand, depleted oil, and gas reservoirs, with their vast storage capacities and  
53 impermeable caprocks, offer a promising solution for hydrogen storage, utilizing existing  
54 infrastructure and drawing upon experiences from methane and CO<sub>2</sub> sequestration [17-19].  
55 However, the translation of these practices to hydrogen underground storage (UHS) is not  
56 straightforward due to hydrogen's unique properties such as lower density, reactivity, and  
57 volatility, which differ markedly from CO<sub>2</sub> and CH<sub>4</sub>. These differences raise concerns about  
58 caprock integrity and containment security, particularly in carbonate and sandstone formations  
59 where chemical, geochemical, and microbial interactions might compromise the storage system  
60 [20, 21].

61 Recent research has focused on wettability of rock-brine-H<sub>2</sub> systems and rock-fluid  
62 interfacial interactions [22-24]. Results generally showed that contact angle increased, whereas  
63 H<sub>2</sub>/rock IFT generally decreased with pressure, salinity, and presence of organic acids [25-27]. On  
64 the other hand, high temperature and nanofluids treatment of rock surfaces were identified as  
65 favorable conditions for enhancing the residual trapping of H<sub>2</sub> in the host-rock (quartz, sandstone,  
66 calcite, carbonate, basalt, and organic-rich shale), and capillary trapping capacities of caprocks  
67 (mica and low total organic carbon shale) [28-31]

68 The geochemical interaction of hydrogen with carbonate and sandstone rocks has also  
69 been fairly investigated, suggesting inert behavior in the latter, thereby supporting the feasibility

70 of sandstone as a storage medium [32, 33]. Most studies have observed only minor geochemical  
71 reactions between H<sub>2</sub> and sandstone under various pressures and temperatures, with implications  
72 for reservoir rock permeability. For instance, Yekta and his co-researchers [32, 33] conducted  
73 numerical and experimental assessment of abiotic reactions due to sandstone-H<sub>2</sub> interactions and  
74 found slight reactions between H<sub>2</sub> and sandstone. The reaction was monitored from 6 weeks to 6  
75 months at pressure of 10 MPa and temperature of 100–200 °C using water saturated and dry  
76 sandstone samples.

77 They further performed core flooding experiments to evaluate the impact of changes in  
78 rock mineralogy on the reservoir rock total permeability at shallow downhole conditions (20 °C,  
79 5.5 MPa), and deep subsurface conditions (45 °C, 10 MPa). Their results showed that relative  
80 permeability curves were same at both experimented conditions due to minor change in viscosity  
81 of H<sub>2</sub> with changing temperature and pressure, compared to CO<sub>2</sub> and N<sub>2</sub>. Flesch et al. [34] assessed  
82 the impacts of injected H<sub>2</sub> on sandstone substrates from Germany, they observed noticeable  
83 alteration in porosity and permeability of Triassic and Permian sandstones samples, but no  
84 occurrence of chemical reactions was observed in Tertiary sandstones after 42 days. These findings  
85 generally indicated that H<sub>2</sub> would likely behaves as inert gas in sandstone formations, suggesting  
86 that successful hydrogen storage in sandstone sites is feasible.

87 Conversely, carbonate minerals have demonstrated a propensity to react with H<sub>2</sub>,  
88 potentially affecting storage integrity. In particular, the presence of iron could accelerate reactions,  
89 leading to the transformation of minerals such as pyrite to pyrrhotite and influencing hydrogen  
90 loss. Specifically, Truche et al. [35] showed that pyrite could play a major role in precipitation of  
91 pyrrhotite in an alkaline surrounding at high temperatures (> 90°C) and elevated pressures (50–  
92 100 bar). They emphasized that interaction between H<sub>2</sub> and the host reservoir rock could be

93 quickened in the presence of Fe. Hassannayebi et al. [36] model predictions suggest that  
94 geochemical interactions are quite slow in the short time, although such reactions could result in  
95 precipitation and dissolution at the long run. They attributed H<sub>2</sub> loss and increased pH to the  
96 reduction of pyrite to pyrrhotite.

97 Bo et al. [37] established from their geochemical model results that H<sub>2</sub> loss from  
98 H<sub>2</sub>/calcite/bacteria interactions is initiated by calcite and not by clay minerals and silicate. They  
99 also reported that the influence of pressure and temperature on H<sub>2</sub> loss in brine solution is  
100 negligible, but that calcite plays a major role in considerable H<sub>2</sub> loss during UHS. Gholami [16]  
101 conducted series of kinetic and thermodynamic geochemical modeling to assess the geochemical  
102 reactions from H<sub>2</sub> injection into porous media. The model results were calibrated against  
103 experimental data to demonstrate that the dissolution of halite, anhydrate and carbonates can take  
104 place in the long term, resulting in hydrogen sulfide formation, as well as calcite precipitation, and  
105 pore structure blockage over time because of scale formation.

106 They proposed that pyrite could reduce to pyrrhotite probably at temperature beyond 90 °C  
107 which could promote hydrogen sulfide formation, even when microbial action is non-existence.  
108 However, halite (scale) formation only commences at the end of 10 years, suggesting that halite  
109 dissolution in porous formation is a very slow phenomenon. In another study, Al-Yaseri et al [17]  
110 reported that gas chromatography could only detect traces of CH<sub>4</sub> (0.018 %), whereas no H<sub>2</sub>S was  
111 spotted from H<sub>2</sub>/shale reaction after 11.5 weeks likely because the reaction temperature and period  
112 was not sufficient for noticeable CH<sub>4</sub> production.

113 Despite these insights, the specific interactions between hydrogen and the clay components  
114 within sandstone formations remain underexplored. This gap is critical, as clay minerals are  
115 prevalent in many potential geological storage sites, and their reactivity with hydrogen could

116 significantly influence the efficacy of UHS. Therefore, this study conducts a detailed assessment  
117 of hydrogen's interaction with clay-rich sandstone to delineate the potential geochemical reactions  
118 that may occur. By comparing computed tomography (CT) scans of clay-rich Bandera gray  
119 sandstone micro-structures with Berea sandstone samples, both before and after exposure to  
120 pressurized hydrogen, we aim to illuminate the changes in pore structure that could inform the  
121 feasibility of hydrogen storage in such geological settings.

122

## 123 **2.0 Materials and methods**

124

125

126

127

128

129

130

131

132

133

134

135

136

137

138

139

Berea and clay-rich Bandera gray sandstones were selected for this study as they are representative of common sandstone formations. The mineral composition of the two samples as identified by X-ray diffraction (XRD), is presented in Table 1. The research grade H<sub>2</sub> gas (99.99% purity) was sourced from Air Liquide Saudi Arabia. The sandstones compositions were determined using a Bruker-AXS D8 instrument (Bruker, Germany) (scanning parameters 0–90°, 2 $\theta$ , accuracy in peak positions  $\leq 0.01$  2 $\theta$ , Bragg–Brentano configuration). To commence the experiments, the core samples (4 by 91.2 mm) were cleansed with methanol-toluene solution (50% each) by aging for 1 day. The samples were then encased in heat-shrink polytetrafluoroethylene (PTFE) jacket to prevent H<sub>2</sub> flow into porous media. Subsequently, the core plugs were positioned in the reaction cell (1 diameter and 12 cm long, 316 stainless steel) and vacuumed for 60 minutes to eliminate air from the system [38].

137

138

139 **Table 1.** XRD identification of Berea and Bandera Gray sandstone samples

<b>Composition</b>	Quartz	Kaolinite	Albite	Dolomite	Microcline	Illite	Muscovite	Clinchlore	Chlorite
<b>Bandera Gray sandstone</b>	58.6	1.9	18.9	4.4	-	4.2	-	10.7	1.1
<b>Berea sandstone</b>	90.2	2.8	-	-	5.8	-	1.1	-	-

140

141           Following this stage, the samples were partially saturated (30%) with sea water (with  
142 composition shown in Table 2) and the 99.99% pure pressurized H<sub>2</sub> was injected at 1500 psi ±1  
143 psi and 75°C ± 0.1 °C for a duration of 75 days. Changes in the rock's pore structures were assessed  
144 using CT scan images taken before and after hydrogen injection. The HeliScan micro-CT  
145 instrument, provided by Thermo Fisher Scientific (Czech Republic), was utilized for the scans.  
146 Pore labelling and grain identification were performed based on the threshold values obtained from  
147 the micro-CT scan tomograms. The image segmentation and filtering were carried out using  
148 PERGEOS SOFTWARE (FEI, Thermo Fisher Scientific).

149

150 **Table 2.**       Composition of seawater brine used for saturating the rock samples

<b>Ions</b>	Na <sup>+</sup>	Ca <sup>2+</sup>	Mg <sup>2+</sup>	SO <sub>4</sub> <sup>2-</sup>	Cl <sup>-</sup>	HCO <sub>3</sub> <sup>-</sup>	Total
<b>Concentration (ppm)</b>	18,300	650	2110	4,290	32,200	120	57,670

151

152           Smoothing and noise removal from the raw data were accomplished using a nonlocal  
153 means filter. Image segmentation was performed using gradient marker-based watershed tool  
154 (PERGEOS SOFTWARE). Porosities in both 2D and 3D were derived from the segmented data  
155 of each core sample. Alterations in the core pore structures were deduced from changes in porosity  
156 observed before and after the injection of pressurized hydrogen into the rock samples. The set of



157 scans—Dry (before H<sub>2</sub> treatment) and after 75 days of H<sub>2</sub> treatment for the Berea and Bandera  
158 Gray sandstones—were processed using PerGeos software (FEI-Thermo Fisher).

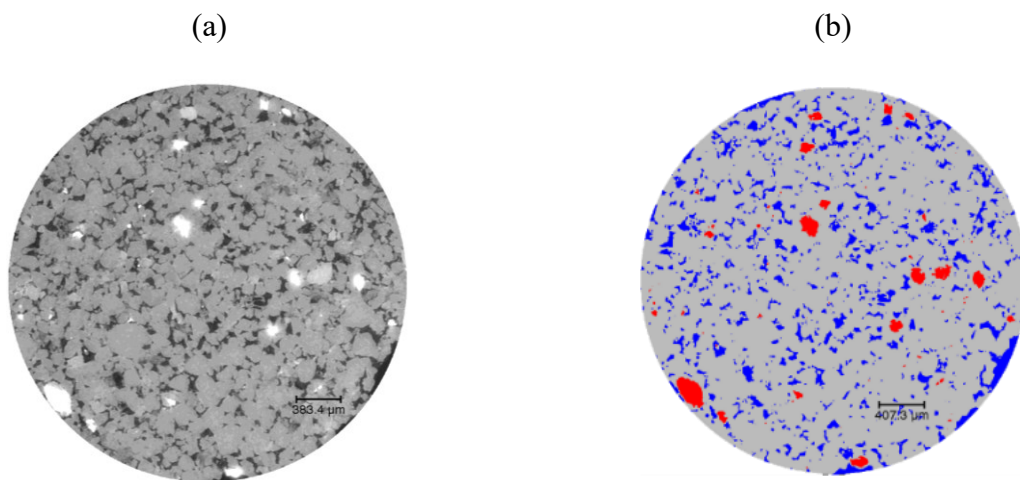
159 This process began by aligning their orientations and registering two images at a time,  
160 using the dry sample scan as the reference. Multiple iterations of the image registration process  
161 were carried out to ensure that unchanged regions of the sample would cancel out in the  
162 differencing step. Normalized mutual information was employed as the metric for image  
163 registration, aiming to minimize entropy between the histograms of the model and reference,  
164 thereby maximizing mutual information. The transformed image was resampled using Lanczos  
165 interpolation.

166 After linearly scaling the attenuation histograms of the 3D registered datasets to match,  
167 their difference was calculated. Gradient Marker-based Watershed and Top-Hat Segmentation  
168 were applied to the image derived from the difference between the pre- and post-treatment images,  
169 enabling the labelling of pores and grains by selecting their thresholds. Subsequently, the volume  
170 fractions of each label were calculated to determine the differences in porosity and clay content.

### 171 **3.0 Result and discussion**

172 Previous research on UHS [33, 37, 39-41] has explored the geochemical and  
173 biochemical interactions between injected hydrogen and the host sandstone during underground  
174 hydrogen storage (UHS), yet the specific reactions involving clay-rich sandstone remain under-  
175 documented in the literature. This study addresses this gap by comparing the interaction of  
176 hydrogen with clay-rich Bandera Gray sandstone to that of Berea sandstone. Presented in Figures  
177 1-8, the results delineate the extent of these interactions. As illustrated in Figures 1-4, the pre- and  
178 post-interaction images exhibit remarkable consistency, indicating negligible geochemical  
179 reaction between the hydrogen and the Berea sandstone matrix.

180 The comparative analysis commenced with the examination of 2D and 3D micro-CT  
181 images of Berea sandstone cores both before and after 75 days of hydrogen exposure. As illustrated  
182 in Fig 1-4, the pre- and post-interaction images exhibit remarkable consistency, indicating  
183 negligible geochemical reaction between the hydrogen and the Berea sandstone matrix. This  
184 observation is further corroborated by the microstructural stability in the micro-CT images, with  
185 negligible changes in pore structure post-injection (see Table 3). For instance, the porosity of Berea  
186 sandstone showed a minimal increase from 11.27% to 11.32%, the clay content altered slightly  
187 from 1.28% to 1.35%, and the grain content exhibited negligible variation, shifting from 87.43%  
188 to 87.57%. These data clearly showed that the injection of pressurized H<sub>2</sub> into the Berea sandstone  
189 demonstrated no significant reaction with the porous medium.

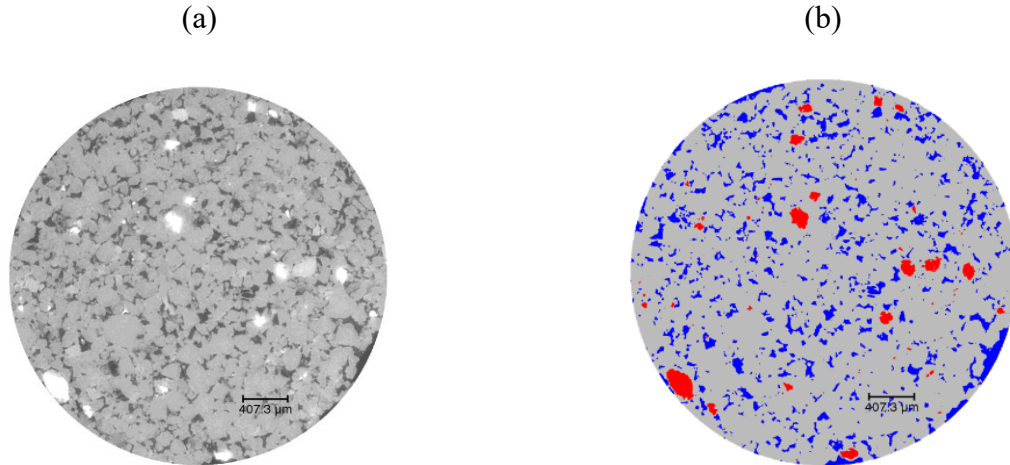


190 **Fig. 1.** Images of Berea sandstone images prior to hydrogen injection, including (a) a 2D raw  
191 image and (b) a 2D segmented image, which establish a baseline for the sandstone's initial  
192 condition.

193

194

195

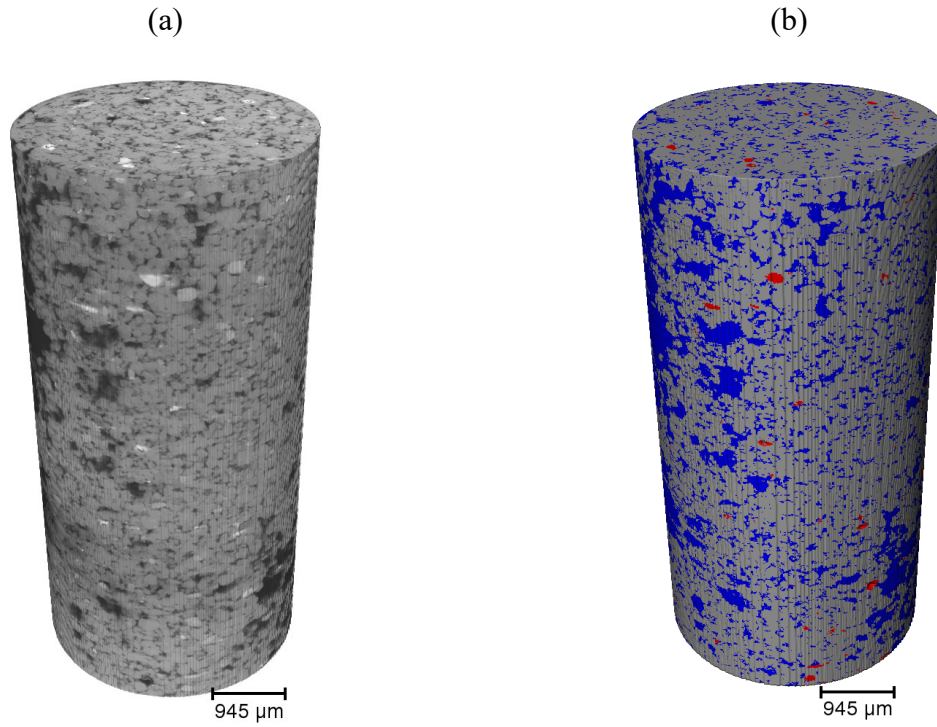


196 **Fig. 2.** Images of Berea sandstone after pressurized H<sub>2</sub> injection showing (a) 2D raw image and  
197 (b) 2D segmented image.

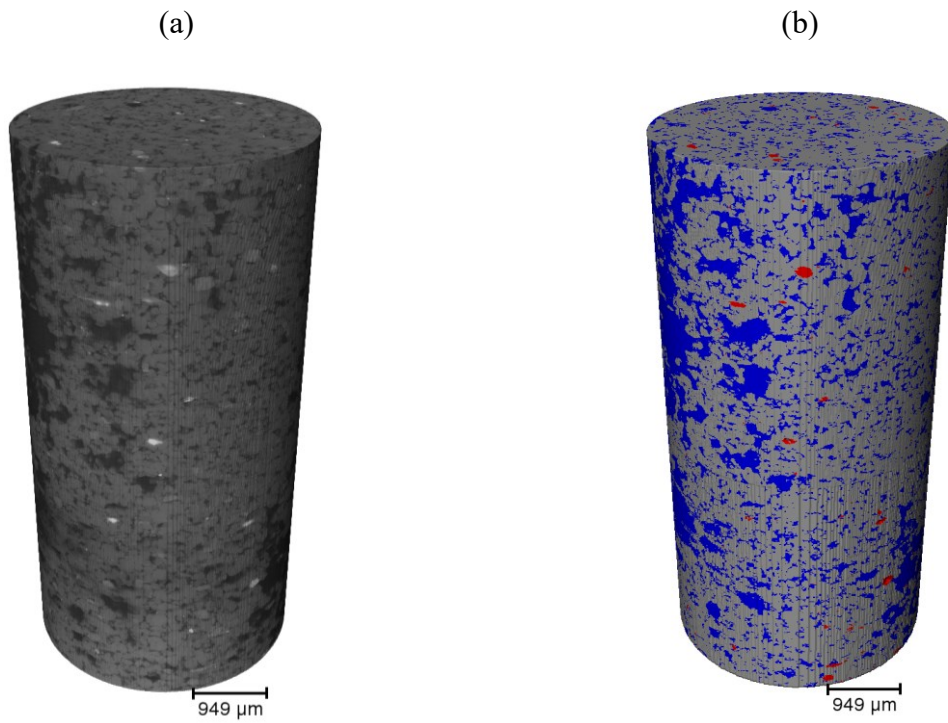
198 Generally, there is a good match between the results reported in literature for sandstone-  
199 H<sub>2</sub> interactions and results obtained in this study. Labus and Tarkowski [42] conducted  
200 geochemical studies to evaluate the possibility of H<sub>2</sub> sub-surface storage in mudstone, claystone,  
201 and sandstone samples from Polish lowlands. Their research highlighted goethite as a primary  
202 mineral in H<sub>2</sub> consumption, with sandstone displaying minimal porosity alteration, especially  
203 when contrasted with mudstone and claystone.

204 Supporting these findings, Yekta et al. [33] posited that limited reaction is expected  
205 between H<sub>2</sub> and sandstone reservoirs. Similarly, Hassanpouryouzband et al. [39] demonstrated  
206 through more than 250 batch reaction experiments that the loss of H<sub>2</sub> from geochemical  
207 interactions between host-sandstone reservoir rock and injected H<sub>2</sub> does not occur during UHS.  
208 This study corroborates the view that sandstone, with its inherent high storage capacity and  
209 resilience to geochemical changes, emerges as a preferable candidate for UHS over carbonate  
210 formations.

211



212 **Fig. 3.** Images of Berea sandstone before pressurized H<sub>2</sub> injection showing (a) 3D raw image and  
213 (b) 3D segmented image.



214

215 **Fig. 4.** Images of Berea sandstone after pressurized H<sub>2</sub> injection showing (a) 3D raw image and  
216 (b) 3D segmented image.

217 **Table 3.** Composition of Berea sandstone before and after H<sub>2</sub> injection

	porosity [%]	Clay [%]	Grains [%]
Berea Sandstone (Before)	11.27	1.28	87.43
Berea Sandstone (After)	11.32	1.35	87.57

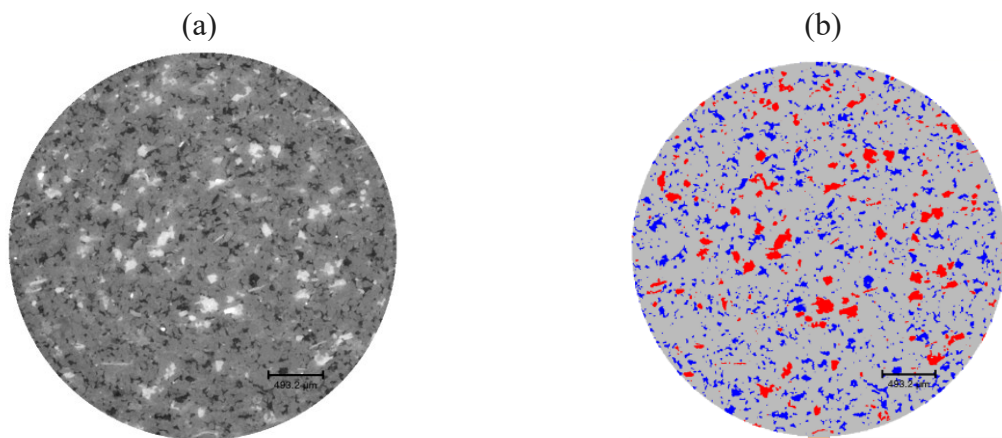
218  
219 Results presented in Figure 5-8 showed that there was no obvious discrepancy between the  
220 2D and 3D images of the clay-rich Bandera Gray sandstone before and after injection of H<sub>2</sub>. The  
221 micro-CT images were further compared with the changes in pore structure shown in Table 4.  
222 Generally, there were no distinct changes in porosity, proportion of clays and grains composition  
223 after the cores were pressurized with H<sub>2</sub>. Porosity of Bandera Gray was 10.16% and 10.23% before  
224 and after interaction with H<sub>2</sub>. Clay composition remained almost unchanged at 4.81% and 4.87%  
225 pre and post H<sub>2</sub> injection respectively whereas there was no significant change in grain percentage  
226 at 85.02% pre hydrogen injection and 85.16% post H<sub>2</sub> injection.

227 Our results generally showed that there is no dissolution or expansion of clays and quartz  
228 composition of the sandstone rocks in the early stages of H<sub>2</sub> injection into Berea sandstone and  
229 clay-rich Bandera Gray sandstone formation. These results are consistent with findings from  
230 previous studies [43, 44]. Ho et al. [43] conducted Nuclear Magnetic Resonance (NMR)  
231 experiments to investigate the NMR response of injected H<sub>2</sub> into Berea sandstone samples. They  
232 observed no adsorption hysteresis in Berea sandstone, suggesting that H<sub>2</sub> loss is unlikely during  
233 UHS in sandstone formation. Similarly, Ho et al. [44] conducted meta-dynamics molecular  
234 simulations to compute the free energy landscape of H<sub>2</sub> intercalation into montmorillonite  
235 interlayers. The simulation prediction showed that H<sub>2</sub> intercalation into hydrated interlayers is

236 thermodynamically unfavorable, suggesting that the loss and leakages of H<sub>2</sub> arising from H<sub>2</sub>  
237 intercalation into clay interlayer during UHS is very limited, if occur at all.

238 With reference to the results obtained in this research, it appears that sandstone formations  
239 with a modest quantity of clay in their structure could be a good alternative for UHS. However, it  
240 is suggested to investigate the interactions between H<sub>2</sub>/brine system and clay rich sandstone for  
241 more than 75 days experimented in this research to ensure that such storage sites are suitable for  
242 geological hydrogen storage for longer period.

243



244

245 **Fig. 5.** Images of Bandera Gray sandstone before pressurized H<sub>2</sub> injection showing (a) 2D raw  
246 image and (b) 2D segmented image.

247

248

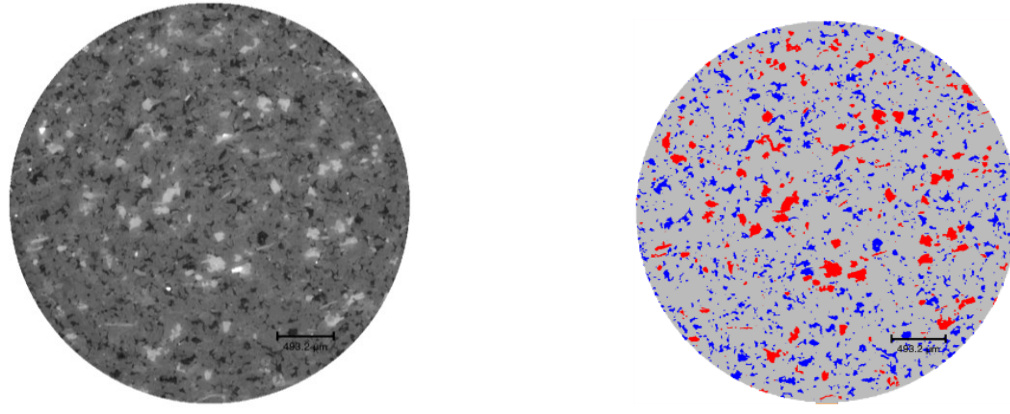
249

250

(a)

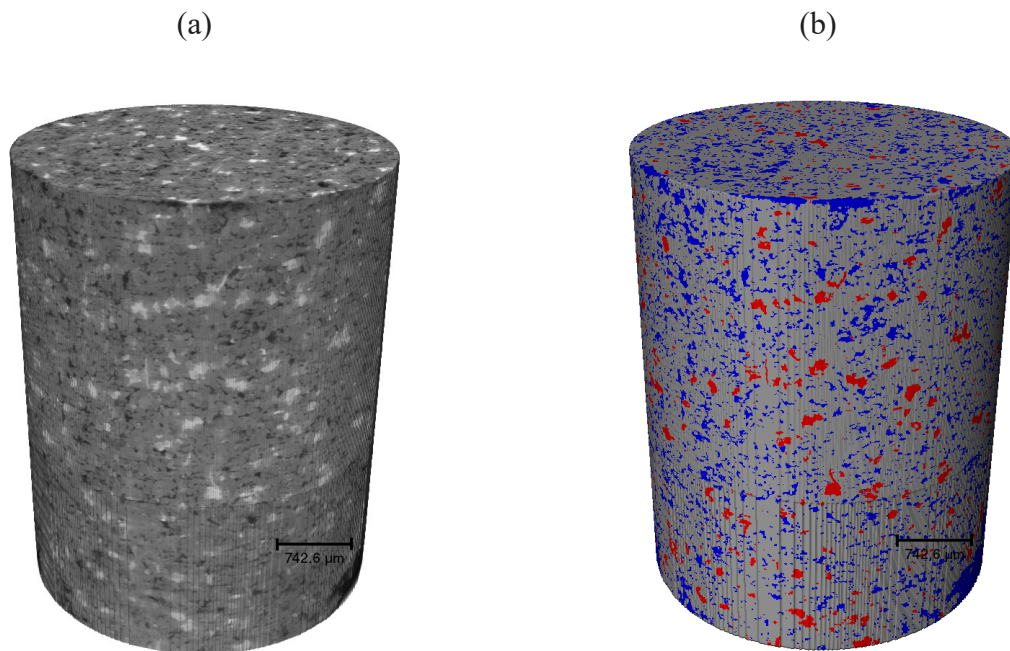
(b)





251

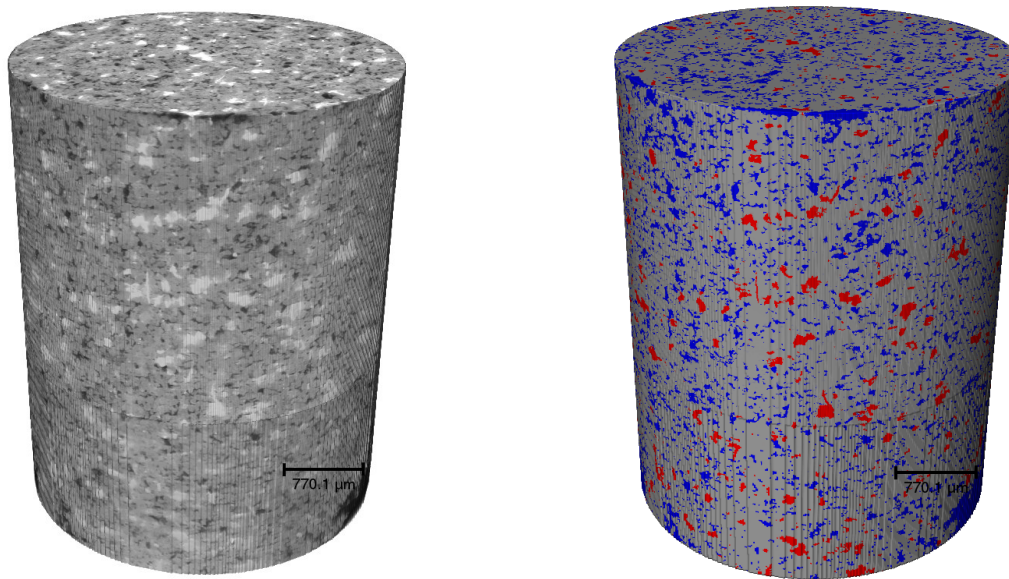
252 **Fig. 6.** Images of Bandera Gray sandstone after pressurized H<sub>2</sub> injection showing (a) 2D raw  
253 image and (b) 2D segmented image.



254 **Fig. 7.** Images of Bandera Gray sandstone before pressurized H<sub>2</sub> injection showing (a) 3D raw  
255 image and (b) 3D segmented image.

	porosity [%]	Clay [%]	Grains [%]
Bandera gray (Before)	10.16	4.81	85.02
Bandera gray (After)	10.23	4.87	85.16

(a) (b)



256 **Fig. 8.** Images of Bandera Gray sandstone after pressurized H<sub>2</sub> injection showing (a) 3D raw image  
 257 and (b) 3D segmented image.

258

#### 259 **4. Conclusions**

260

261

262

263

264

265

266

267

Sandstone formations are increasingly recognized as favorable geo-storage media for geological hydrogen storage. However, a comprehensive understanding of the rock/brine/H<sub>2</sub> interactions is imperative to determine their suitability for UHS. Prior investigations into these reactions have indicated negligible interactions between hydrogen and sandstone minerals. Building on prior research, our study uniquely examines the impact of clay content in Berea and Bandera Gray sandstones on H<sub>2</sub>/brine/rock interactions during geological hydrogen storage, an



268 aspect previously underexplored. We simulated downhole conditions by injecting pressurized  
269 hydrogen into brine-saturated cores at 75°C and 1500 psi over a period of 75 days, utilizing micro-  
270 computed tomography to analyze the core samples' pore structures and morphology before and  
271 after treatment.

272

273         The experiments revealed no discernible morphological changes or porosity alterations in  
274 Berea and Bandera Gray sandstones, underscoring the inert nature of sandstone—even with a  
275 substantial clay presence—when interacting with hydrogen. Our findings suggest that clay-rich  
276 sandstone formations offer a more stable option for hydrogen storage than previously thought,  
277 paving the way for more efficient and sustainable energy storage solutions. Accordingly, we  
278 conclude that clay-rich sandstone formations are promising candidates for hydrogen storage. The  
279 potential for injectivity impairment or clay precipitation appears minimal within the short-term  
280 storage duration assessed. These findings hold significant potential for enhancing our  
281 understanding and selection of optimal porous media for industrial-scale hydrogen storage. Given  
282 the minimal changes observed in the sandstone formations, our research indicates that these  
283 materials could be effectively utilized in industrial-scale hydrogen storage, supporting the  
284 transition to cleaner energy sources.

285

## 286 **References**

287

288 [1] O.C. Anika, S.G. Nnabuife, A. Bello, E.R. Okoroafor, B. Kuang, R. Villa, Prospects of low  
289 and zero-carbon renewable fuels in 1.5-degree net zero emission actualisation by 2050: A critical  
290 review, *Carbon Capture Science & Technology* 5 (2022) 100072.

- 291 [2] J. Dixon, K. Bell, S. Brush, Which way to net zero? a comparative analysis of seven UK 2050  
292 decarbonisation pathways, *Renewable and Sustainable Energy Transition* 2 (2022) 100016.
- 293 [3] K. Oshiro, S. Fujimori, Role of hydrogen-based energy carriers as an alternative option to  
294 reduce residual emissions associated with mid-century decarbonization goals, *Applied Energy* 313  
295 (2022) 118803.
- 296 [4] H. Kojima, K. Nagasawa, N. Todoroki, Y. Ito, T. Matsui, R. Nakajima, Influence of renewable  
297 energy power fluctuations on water electrolysis for green hydrogen production, *international  
298 journal of hydrogen energy* 48(12) (2023) 4572-4593.
- 299 [5] F. Alhammad, M. Ali, N.P. Yekeen, M. Ali, H. Hoteit, S. Iglauer, A. Keshavarz, Effect of  
300 methylene blue on wetting characteristics of quartz/H<sub>2</sub>/brine systems: Implication for hydrogen  
301 geological storage, *Journal of Energy Storage* 72 (2023) 108340.
- 302 [6] Q. Hassan, A.M. Abdulateef, S.A. Hafedh, A. Al-samari, J. Abdulateef, A.Z. Sameen, H.M.  
303 Salman, A.K. Al-Jiboory, S. Wieteska, M. Jaszczur, Renewable energy-to-green hydrogen: A  
304 review of main resources routes, processes and evaluation, *International Journal of Hydrogen  
305 Energy* (2023).
- 306 [7] V. Panchenko, Y.V. Daus, A. Kovalev, I. Yudaev, Y.V. Litti, Prospects for the production of  
307 green hydrogen: Review of countries with high potential, *International Journal of Hydrogen  
308 Energy* 48(12) (2023) 4551-4571.
- 309 [8] L. Guo, J. Su, Z. Wang, J. Shi, X. Guan, W. Cao, Z. Ou, Hydrogen safety: An obstacle that  
310 must be overcome on the road towards future hydrogen economy, *International Journal of  
311 Hydrogen Energy* (2023).

- 312 [9] H. Liang, T. Wang, Z. Luo, J. Yu, W. Yi, F. Cheng, J. Zhao, X. Yan, J. Deng, J. Shi,  
313 Investigation on the lower flammability limit and critical inhibition concentration of hydrogen  
314 under the influence of inhibitors, *Fuel* 356 (2024) 129595.
- 315 [10] K.M. Groth, A. Al-Douri, Hydrogen safety, risk, and reliability analysis, *Hydrogen Economy*,  
316 Elsevier 2023, pp. 487-510.
- 317 [11] S.T. Le, T.N. Nguyen, S. Linforth, T.D. Ngo, Safety investigation of hydrogen energy storage  
318 systems using quantitative risk assessment, *International Journal of Hydrogen Energy* 48(7) (2023)  
319 2861-2875.
- 320 [12] Z. Tariq, M. Ali, N. Yekeen, A. Baban, B. Yan, S. Sun, H. Hoteit, Enhancing wettability  
321 prediction in the presence of organics for hydrogen geo-storage through data-driven machine  
322 learning modeling of rock/H<sub>2</sub>/brine systems, *Fuel* 354 (2023) 129354.
- 323 [13] H. Aghaei, A. Al-Yaseri, A. Toorajipour, B. Shahsavani, N. Yekeen, K. Edlmann, Host-rock  
324 and caprock wettability during hydrogen drainage: Implications of hydrogen subsurface storage,  
325 *Fuel* 351 (2023) 129048.
- 326 [14] R. Ershadnia, M. Singh, S. Mahmoodpour, A. Meyal, F. Moeini, S.A. Hosseini, D.M.  
327 Sturmer, M. Rasoulzadeh, Z. Dai, M.R. Soltanian, Impact of geological and operational conditions  
328 on underground hydrogen storage, *International Journal of Hydrogen Energy* 48(4) (2023) 1450-  
329 1471.
- 330 [15] L. Lankof, K. Urbańczyk, R. Tarkowski, Assessment of the potential for underground  
331 hydrogen storage in salt domes, *Renewable and Sustainable Energy Reviews* 160 (2022) 112309.
- 332 [16] R. Gholami, Hydrogen storage in geological porous media: Solubility, mineral trapping, H<sub>2</sub>S  
333 generation and salt precipitation, *Journal of Energy Storage* 59 (2023) 106576.

- 334 [17] A. Al-Yaseri, H. Al-Mukainah, N. Yekeen, Experimental insights into limestone-hydrogen  
335 interactions and the resultant effects on underground hydrogen storage, *Fuel* 344 (2023) 128000.
- 336 [18] A. Al-Yaseri, H. Al-Mukainah, N. Yekeen, A.S. Al-Qasim, Experimental investigation of  
337 hydrogen-carbonate reactions via computerized tomography: Implications for underground  
338 hydrogen storage, *International Journal of Hydrogen Energy* 48(9) (2023) 3583-3592.
- 339 [19] A. Hassanpouryouzband, E. Joonaki, K. Edlmann, R.S. Haszeldine, Offshore geological  
340 storage of hydrogen: is this our best option to achieve net-zero?, *ACS Energy Letters* 6(6) (2021)  
341 2181-2186.
- 342 [20] N. Liu, A.R. Kavscek, M.A. Fernø, N. Dopffel, Pore-scale study of microbial hydrogen  
343 consumption and wettability alteration during underground hydrogen storage, *Frontiers in Energy*  
344 *Research* 11 (2023) 1124621.
- 345 [21] A. Aftab, A. Al-Yaseri, A. Nzila, J. Al Hamad, A.O. Amao, M. Sarmadivaleh, Quartz–H<sub>2</sub>–  
346 brine bacterium wettability under realistic geo-conditions: towards geological hydrogen storage,  
347 *Energy & Fuels* 37(7) (2023) 5623-5631.
- 348 [22] M. Aslannezhad, M. Ali, A. Kalantariasl, M. Sayyafzadeh, Z. You, S. Iglauer, A. Keshavarz,  
349 A review of hydrogen/rock/brine interaction: Implications for Hydrogen Geo-storage, *Progress in*  
350 *Energy and Combustion Science* 95 (2023) 101066.
- 351 [23] A. Alanazi, H.R. Abid, M. Usman, M. Ali, A. Keshavarz, V. Vahrenkamp, S. Iglauer, H.  
352 Hoteit, Hydrogen, carbon dioxide, and methane adsorption potential on Jordanian organic-rich  
353 source rocks: Implications for underground H<sub>2</sub> storage and retrieval, *Fuel* 346 (2023) 128362.
- 354 [24] A. Alanazi, M. Ali, M. Mowafi, H. Hoteit, Effect of organics and nanofluids on capillary-  
355 sealing efficiency of caprock for hydrogen and carbon-dioxide geological storage,

356 ARMA/DGS/SEG International Geomechanics Symposium, ARMA, 2022, pp. ARMA-IGS-  
357 2022-009.

358 [25] M. Ali, N. Yekeen, N. Pal, A. Keshavarz, S. Iglauer, H. Hoteit, Influence of organic molecules  
359 on wetting characteristics of mica/H<sub>2</sub>/brine systems: Implications for hydrogen structural trapping  
360 capacities, *Journal of Colloid and Interface Science* 608 (2022) 1739-1749.

361 [26] A. Alanazi, N. Yekeen, M. Ali, M. Ali, I.S. Abu-Mahfouz, A. Keshavarz, S. Iglauer, H. Hoteit,  
362 Influence of organics and gas mixing on hydrogen/brine and methane/brine wettability using  
363 Jordanian oil shale rocks: Implications for hydrogen geological storage, *Journal of Energy Storage*  
364 62 (2023) 106865.

365 [27] M. Hosseini, M. Ali, J. Fahimpour, A. Keshavarz, S. Iglauer, Assessment of rock-hydrogen  
366 and rock-water interfacial tension in shale, evaporite and basaltic rocks, *Journal of Natural Gas*  
367 *Science and Engineering* 106 (2022) 104743.

368 [28] N. Yekeen, A. Al-Yaseri, B.M. Negash, M. Ali, A. Giwelli, L. Esteban, J. Sarout, Clay-  
369 hydrogen and clay-cushion gas interfacial tensions: Implications for hydrogen storage,  
370 *International Journal of Hydrogen Energy* 47(44) (2022) 19155-19167.

371 [29] M. Hosseini, J. Fahimpour, M. Ali, A. Keshavarz, S. Iglauer, H<sub>2</sub>- brine interfacial tension as  
372 a function of salinity, temperature, and pressure; implications for hydrogen geo-storage, *Journal*  
373 *of Petroleum Science and Engineering* 213 (2022) 110441.

374 [30] F. Alhamad, R. Sedev, M. Ali, M. Ali, H. Hoteit, S. Iglauer, A. Keshavarz, Effect of methyl  
375 orange on the hydrogen wettability of sandstone formation for enhancing the potential of  
376 underground hydrogen storage, *Energy & Fuels* 37(8) (2023) 6149-6157.

377 [31] M. Hosseini, M. Ali, J. Fahimpour, A. Keshavarz, S. Iglauer, Basalt-H<sub>2</sub>-brine wettability at  
378 geo-storage conditions: Implication for hydrogen storage in basaltic formations, *Journal of Energy*  
379 *Storage* 52 (2022) 104745.

380 [32] A. Ebrahimiyeqta, Characterization of geochemical interactions and migration of hydrogen  
381 in sandstone sedimentary formations: application to geological storage, Université d'Orléans,  
382 2017.

383 [33] A.E. Yekta, M. Pichavant, P. Audigane, Evaluation of geochemical reactivity of hydrogen in  
384 sandstone: Application to geological storage, *Applied Geochemistry* 95 (2018) 182-194.

385 [34] S. Flesch, D. Pudlo, D. Albrecht, A. Jacob, F. Enzmann, Hydrogen underground storage—  
386 Petrographic and petrophysical variations in reservoir sandstones from laboratory experiments  
387 under simulated reservoir conditions, *International Journal of Hydrogen Energy* 43(45) (2018)  
388 20822-20835.

389 [35] L. Truche, G. Joubert, M. Dargent, P. Martz, M. Cathelineau, T. Rigaudier, D. Quirt, Clay  
390 minerals trap hydrogen in the Earth's crust: evidence from the Cigar Lake uranium deposit,  
391 Athabasca, *Earth and Planetary Science Letters* 493 (2018) 186-197.

392 [36] N. Hassannayebi, S. Azizmohammadi, M. De Lucia, H. Ott, Underground hydrogen storage:  
393 application of geochemical modelling in a case study in the Molasse Basin, Upper Austria,  
394 *Environmental Earth Sciences* 78 (2019) 1-14.

395 [37] Z. Bo, L. Zeng, Y. Chen, Q. Xie, Geochemical reactions-induced hydrogen loss during  
396 underground hydrogen storage in sandstone reservoirs, *International Journal of Hydrogen Energy*  
397 46(38) (2021) 19998-20009.

398 [38] A. Al-Yaseri, A. Fatah, A. Amao, D. Wolff-Boenisch, Basalt–Hydrogen–Water Interactions  
399 at Geo-Storage Conditions, *Energy & Fuels* (2023).

400 [39] A. Hassanpouryouzband, K. Adie, T. Cowen, E.M. Thaysen, N. Heinemann, I.B. Butler, M.  
401 Wilkinson, K. Edlmann, Geological hydrogen storage: geochemical reactivity of hydrogen with  
402 sandstone reservoirs, *ACS Energy Letters* 7(7) (2022) 2203-2210.

403 [40] L. Zeng, S. Vialle, J. Ennis-King, L. Esteban, M. Sarmadivaleh, J. Sarout, J. Dautriat, A.  
404 Giwelli, Q. Xie, Role of geochemical reactions on caprock integrity during underground hydrogen  
405 storage, *Journal of Energy Storage* 65 (2023) 107414.

406 [41] C. Hemme, W. Van Berk, Hydrogeochemical Modeling to Identify Potential Risks of  
407 Underground Hydrogen Storage in Depleted Gas Fields, *Applied Sciences* 8(11) (2018) 2282.

408 [42] K. Labus, R. Tarkowski, Modeling hydrogen–rock–brine interactions for the Jurassic  
409 reservoir and cap rocks from Polish Lowlands, *International Journal of Hydrogen Energy* 47(20)  
410 (2022) 10947-10962.

411 [43] T.A. Ho, S.T. Dang, N. Dasgupta, A. Choudhary, C.S. Rai, Y. Wang, Nuclear magnetic  
412 resonance and molecular simulation study of H<sub>2</sub> and CH<sub>4</sub> adsorption onto shale and sandstone for  
413 hydrogen geological storage, *International Journal of Hydrogen Energy* (2023).

414 [44] T.A. Ho, C.F. Jove-Colon, Y. Wang, Low hydrogen solubility in clay interlayers limits gas  
415 loss in hydrogen geological storage, *Sustainable Energy & Fuels* (2023).

416